RESEARCH FRONT

CSIRO PUBLISHING

Environ. Chem.
http://dx.doi.org/10.1071/EN11168

Research Paper

Effect of aqueous-phase processing on aerosol chemistry and size distributions in Fresno, California, during wintertime

Xinlei Ge,[A] *Qi Zhang,*[A,D] *Yele Sun,*[B] *Christopher R. Ruehl*[C] *and Ari Setyan*[A]

[A]Department of Environmental Toxicology, University of California, One Shields Avenue, Davis, CA 95616, USA.
[B]State Key Laboratory of Atmospheric Boundary Layer Physics and Atmospheric Chemistry, Institute of Atmospheric Physics, Chinese Academy of Sciences, Beijing 100029, P. R. China.
[C]Environmental Science, Policy, and Management. University of California, 130 Mulford Hall, Berkeley, CA 94720, USA.
[D]Corresponding author. Email: dkwzhang@ucdavis.edu

Environmental context. Aqueous-phase processes in fogs and clouds can significantly alter atmospheric fine particles with consequences for climate and human health. We studied the influence of fog and rain on atmospheric aerosol properties, and show that aqueous-phase reactions contribute to the production of secondary aerosol species and change significantly the composition and microphysical properties of aerosols. In contrast, rains effectively remove aerosols and reduce their concentrations.

Abstract. Submicrometre aerosols (PM_1) were characterised in situ with a high resolution time-of-flight aerosol mass spectrometer and a scanning mobility particle sizer in Fresno, CA, from 9 to 23 January 2010. Three dense fog events occurred during the first week of the campaign whereas the last week was influenced by frequent rain events. We thus studied the effects of aqueous-phase processing on aerosol properties by examining the temporal variations of submicrometre aerosol composition and size distributions. Rains removed secondary species effectively, leading to low loadings of PM_1 dominated by primary organic species. Fog episodes, however, increased the concentrations of secondary aerosol species (sulfate, nitrate, ammonium and oxygenated organic aerosol). The size distributions of these secondary species, which always showed a droplet mode peaking at ~500 nm in the vacuum aerodynamic diameter, increased in mode size during fog episodes as well. In addition, the oxygen-to-carbon ratio of oxygenated organic species increased in foggy days, indicating that fog processing likely enhances the production of secondary organic aerosol as well as its oxidation degree. Overall, our observations show that aqueous-phase processes significantly affect submicrometre aerosol chemistry and microphysics in the Central Valley of California during winter, responsible for the production of secondary inorganic and organic aerosol species and the formation of droplet mode particles, thus altering the climatic and health effects of ambient aerosols in this region.

Additional keywords: Aerodyne high-resolution time-of-flight aerosol mass spectrometer (HR-ToF-AMS), aqueous-phase reaction, fog/cloud processing, SOA production, submicrometre aerosol chemistry.

Received 23 December 2011, accepted 10 May 2012, published online 26 June 2012

Introduction

Atmospheric particulate matter (PM) plays important roles in many environmental issues. It influences the radiative balance of the Earth's climate system directly by absorbing and scattering solar and thermal radiation and indirectly through affecting cloud formation and cloud properties.[1] Airborne particles are also of concern for their adverse effects on human health[2] and ecosystems.[3] The various effects of ambient particles are controlled by their concentrations, compositions, size distributions and other physical and chemical properties. Aqueous-phase processes involving fog, cloud, precipitation and aerosol water may significantly influence these properties. On the one hand, water droplets enhance the removal of aerosol and its gaseous precursors from the atmosphere; on the other hand, airborne droplets and water-containing aerosols provide media for dissolution of gas species, aqueous-phase reactions and production of secondary aerosol species (i.e. low volatility species that remain in the particle phase after water evaporation). A quantitative understanding of the influence of aqueous-phase processing on aerosol chemistry is thus important for addressing issues related to PM pollution and its effects.

The PM levels in the San Joaquin Valley (SJV) – the southern part of the Central Valley of California – often exceed the national ambient air quality standards.[4] The valley also frequently experiences widespread, persistent regional radiation

fogs during wintertime, owing to its unique geographical features and meteorological conditions.[5] Early studies on SJV fog or cloud chemistry focussed on the characteristics of inorganic species in fog waters,[6,7] with a few reports on measurements of carboxylic acids and carbonyls.[8–11] These studies showed that fogs can effectively scavenge secondary inorganic aerosol species and their gaseous precursors and that the production of sulfate can be enhanced significantly by fog processing. The production of nitrate from nitrogen oxides (NO_x), however, was found generally insignificant in fogs.[12] In the past decades, changes in the chemical composition of the atmosphere due to significant reductions of regional emissions may have largely altered fog chemistry in this region. For example, slower production of sulfate was observed during winter fogs in 1995 compared to observations in the 1980s, because of lowered sulfur dioxide (SO_2) concentration in this area and lack of oxidants inside the fog layer.[13] As a result, nitrate and ammonium have become dominant components in fog drops in California.[14,15]

In recent years, studies on fog chemistry have given increasing attention to organic species. Dissolved organic species, including aromatic carbonyls,[16,17] phenols and nitrophenols,[18] carboxylic acids,[14,19,20] amino compounds,[21–23] humic-like substances[24,25] and various other species[26–31] were studied in detail in fog waters. Specifically, comprehensive characterisation of organic matter in Davis[32] and Fresno fog waters[33,34] led to the identification of hundreds of organic species with a variety of functional groups, including organic acids, amines, nitrosamines, organosulfur compounds, organic nitrates and oxygenated species. Although these studies have increased our understanding of the composition of organic matter in fog drops and aerosols, the production and removal of different fine particulate organic compounds in the atmosphere remain poorly understood. More work is needed to elucidate the scavenging processes of carbonaceous particles originating from different source types and to determine the significance of secondary organic aerosol (SOA) formation due to aqueous-phase reaction pathways.[5]

Previous studies on aerosol–fog interactions mainly analysed fog water and aerosol compositions off-line, and lacked detailed real-time information on the characteristics and temporal variations of interstitial aerosols, especially those in the submicrometre size range (PM_1, i.e. particles with an aerodynamic diameter less than 1 μm). As PM_1 account for a major fraction of fine aerosols that have serious effects on human health[35] and climate[36] a quantitative understanding of fog processing on PM_1 is essential. Aerodyne aerosol mass spectrometer (AMS) systems have been deployed around the world to characterise quantitatively the composition and size distribution of PM_1.[37–39] The AMS data can also provide valuable information on the sources and processes of organic aerosols (OA) through advanced data analyses using factor analysis techniques.[40] This instrument, together with other on-line equipment, was used for characterising PM_1 and studying SOA production during a fog event in London.[41] In addition, an AMS study conducted north of San Francisco, CA, found that interstitial particle mass concentrations reached a maximum under foggy conditions.[42] These observations of enhanced PM_1 concentrations in fog are to the contrary of those from past studies, which often reported the overall reductions of aerosol concentrations during fog episodes.[13,43] Therefore, the effect of fog processing on submicrometre aerosol chemistry deserves more in-depth investigations.

In this study, we report the characterisation of submicrometre particles using an Aerodyne high-resolution time-of-flight aerosol mass spectrometer (HR-ToF-AMS) and a scanning mobility particle sizer (SMPS) during a field campaign operated in winter 2010 in Fresno, California. This study was part of the Aerosol Inhalation Toxicology project supported by the San Joaquin Valley Aerosol Health Effects Center at the University of California at Davis (http://saherc.ucdavis.edu/, accessed 3 June 2012). A main objective of the project was to investigate the mechanistic links between ambient particles and the health effects that they elicit.[4,44–47] During this campaign, dense fog events and persistent precipitation occurred, and in this paper, we focus on the effects of fog and rain on submicrometre aerosol chemistry. We first present an overview of the PM_1 characteristics and then discuss in detail the effects of fog processing and rain scavenging on different aerosol species.

Experimental methods

Sampling site and instrumentation

Fresno is located in the central region of the SJV, at ~200 miles (~322 km) north of Los Angeles, 170 miles (~274 km) south of the state capital, Sacramento, and 160 miles (~257 km) east of the Pacific Ocean coast. With a population of ~500 000, Fresno is the largest city in the SJV. Our sampling site (36°48′35.26″N, 119°46′42.00″W) was located at the University of California Center at Fresno, ~600 m east of a highway (Yosemite FWY-41), bounded by residences to the north and a commercial centre to the south across the principal arterial road – Shaw Avenue (Fig. 1).

From 9 to 23 January 2010, a HR-ToF-AMS (Aerodyne Inc., Billerica, MA) and a SMPS (TSI Inc., Shoreview, MN) were deployed to characterise ambient particles in real time, with time resolutions of 5–10 min. A $PM_{2.5}$ cyclone (URG Corp., Chapel Hill, NC) was placed at the inlet of the sampling line to remove particles (and droplets) larger than 2.5 μm in aerodynamic diameter and a diffusion dryer was used to remove moisture in the aerosols before SMPS analyses. The relative humidity (RH) of aerosols sampled by the HR-ToF-AMS, which was measured by a RH probe mounted directly in front of the AMS inlet, was 33 % on average (range: 20–60 %) during this study, indicating that the particles sampled into the AMS were overall dry. The HR-ToF-AMS measures the size-resolved chemical composition of non-refractory submicrometre particles (NR-PM_1) using thermal evaporation (~600 °C) and 70 eV electron ionisation (EI) mass spectrometry.[48] The mass spectrometer switched between 'V' mode and 'W' mode every 5 min, allowing for both highly sensitive quantification of individual species (detection limits of V-mode were ~10 ng m^{-3}) and improved chemical resolution for organic analysis (mass resolution of W-mode was ~5000 in this study).[49] Under V-mode operation, the HR-ToF-AMS also cycled through the mass spectrum mode and the particle time-of-flight (PToF) mode every 15 s, spending 6 and 9 s on each.

The HR-ToF-AMS was calibrated for particle sizing using both pure ammonium nitrate and standard polystyrene latex (PSL) spheres (Duke Scientific Corp., Palo Alto, CA) generated from aqueous solutions using a collision atomiser, across the diameter range of 100–700 nm before the start of the campaign. The calibrations of ionisation efficiency (IE) were performed before, during, and at the end of the campaign using size-selected monodisperse pure ammonium nitrate particles. The standard procedures for the size and IE calibrations are given

Fig. 1. A map of the sampling site (red star) and its surroundings.

elsewhere.[48] The detection limits (DLs) of the AMS were determined as 3 times the standard deviations (3σ) of the measured values in particle-free ambient air sampled through a high efficiency particulate air (HEPA) filter.[50] The filtered air measurement was conducted in the middle of the campaign (1600–1700 hours on 18 January). The 5-min DLs for organics, sulfate, nitrate, ammonium and chloride were determined at 60, 11, 8, 30 and 12 ng m^{-3} for V-mode measurements. The propagated 5-min DL for total NR-PM_1 (organics + sulfate + nitrate + ammonium + chloride) was 0.06 μg m^{-3}.

HR-AMS data analysis

The HR-ToF-AMS data were analysed using the standard ToF-AMS analysis toolkit *SQUIRREL v1.51H* and the *PIKA module v1.10H* (downloaded from: http://cires.colorado.edu/jimenez-group/ToFAMSResources/ToFSoftware/index.html, accessed 3 June 2012) written in *Igor Pro 6.22A* (Wavemetrics, Portland, OR, USA). The raw mass spectra were processed using the standard fragmentation table described by Allan et al.[51] with a few adjustments based on data recorded during the filtered air period (e.g. the $^{16}O^+$ to $^{14}N^+$ ratio for air signal and the subtraction of gaseous contributions to the measured CO_2^+ signal). In addition, the signals of H_2O^+ and CO^+ for organics were not directly measured but scaled to that of CO_2^+ based on the fragmentation patterns proposed for ambient aerosols[52]: $CO^+ = CO_2^+$ and $H_2O^+ = 0.225 \times CO_2^+$. The fragmentation pattern of H_2O^+ was determined based on the fragmentation pattern of the background water signal: $HO^+ = 0.229 \times H_2O^+$ and $O^+ = 0.0487 \times H_2O^+$.

A collection efficiency (CE) of 0.5 was introduced to account for the incomplete transmission and detection of particles by the HR-ToF-AMS during this study. This value is consistent with observations from many ambient AMS studies.[48] Recently, Middlebrook et al.[53] evaluated the dependency of CE on aerosol composition and concluded that the CE of acidic particles or particles with a high nitrate fraction (e.g. NH_4NO_3 > 40 % of PM_1) may increase, whereas the CE of dry particles doesn't show significant change with the organic fractions. As presented in the section 'Overview of aerosol characteristics', NR-PM_1 during this study were overall fully neutralised and the mass fraction of NH_4NO_3 was normally below 40 %, supporting the use of CE = 0.5. As shown in Fig. 2a, the SMPS-measured particle volume correlated well with the AMS-measured total mass ($R^2 = 0.90$) and the correlation was independent of the RH in aerosols (Fig. 2b). In addition, the mass-based aerosol size distributions measured by the HR-ToF-AMS (Fig. 2c) also showed similar evolution patterns as the particle volume distributions (calculated assuming spherical particles) measured by the SMPS (Fig. 2d). Note that the discrepancies in the observed size distributions between these two instruments may be due to time-dependent variations in particle density and the presence of irregularly shaped particles.[50] This is because the AMS and the SMPS respond differently to particle density and particle shape.[54] For example, whereas the AMS-measured D_{va} is proportional to particle density, the SMPS-measured mobility diameter (D_m) is independent of it.[54] In addition, as a particle becomes less spherical, the AMS reports smaller D_{va} whereas the SMPS reports larger D_m.[54]

Despite tight correlation, the intercomparison of the AMS mass *v.* the SMPS volume yields a slope of 2.04 g cm^{-3} (Fig. 2b), significantly higher than the average dry NR-PM_1 density of ~1.3 g cm^{-3} estimated for this study based on measured particle composition,[50] which consists of ~26 % ammonium nitrate (density = 1.72 g cm^{-3}), ~4.4 % ammonium sulfate (density = 1.77 g cm^{-3}), ~2.3 % ammonium chloride (density = 1.52 g cm^{-3}), ~38 % primary organic aerosol (POA, density = 1.0 g cm^{-3}) and ~29 % SOA (density = 1.27 g cm^{-3})[55] (Table 1). The slope would be even higher if the masses of black carbon (BC), which was not measured during this study, were accounted for. Possible explanations for this discrepancy include loss of particles in the diffusion dryer connected to the SMPS and the difference between the two instruments in their maximum transmission sizes (e.g. the upper limit of the cut-off size of SMPS is ~700 nm whereas the AMS has partial transmission for particles up to ~2.5 μm[48]). Overall, the good correlation between the AMS and SMPS loading and size distribution data support the use of CE = 0.5 for this dataset. The relative ionisation efficiencies (RIEs)[48]

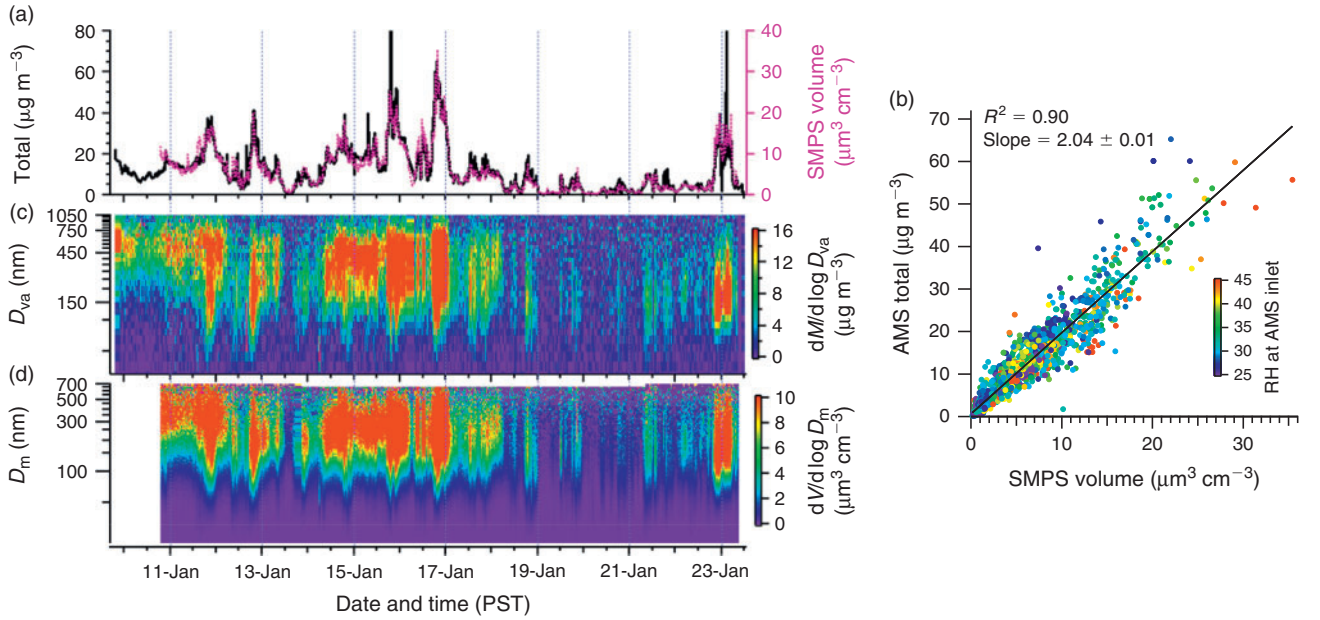

Fig. 2. (a) Comparisons between total non-refractory submicrometre particles (NR-PM_1) mass (organics + sulfate + nitrate + ammonium + chloride) measured by the high resolution time-of-flight aerosol mass spectrometer (HR-ToF-AMS) *v.* apparent particle volume (calculated assuming spherical particles) measured by the scanning mobility particle sizer (SMPS), (b) scatter plot of the total NR-PM_1 mass *v.* SMPS volume (data points are coloured by the relative humidity recorded at the AMS inlet), and temporal variations of the size distribution of (c) PM_1 mass and (d) SMPS volume. Note that the AMS size distribution data was recorded in vacuum aerodynamic diameter (D_{va}) and the SMPS size data was in mobility diameter (D_m). For a spherical particle, $D_{va} = D_m \times$ particle density. (PST, Pacific Standard Time.)

Table 1. Average (±1σ) mass concentrations (μg m^{-3}) of PM_1 species and their fractional contributions (±σ) to the total NR-PM_1 mass from 2100 to 1100 hours in the morning of the 2nd day during the fog, 'other' and rain periods as marked in Fig. 3

The values for the entire study are also listed. POA, primary organic aerosol; OOA, oxygenated organic aerosol

Periods		NR-PM_1	Ammonium	Nitrate	Sulfate	Chloride	POA	OOA
Fog	Concentration	14.2 ± 3.7	1.81 ± 0.30	4.48 ± 0.89	0.76 ± 0.28	0.19 ± 0.10	2.10 ± 1.40	4.91 ± 1.20
	Fraction		12.7 ± 2.1 %	31.4 ± 6.2 %	5.3 ± 2.0 %	1.3 ± 0.7 %	14.7 ± 9.8 %	34.6 ± 8.4 %
'Other'	Concentration	15.3 ± 11.1	1.15 ± 0.89	3.08 ± 2.35	0.38 ± 0.37	0.26 ± 0.28	6.06 ± 6.35	4.38 ± 2.67
	Fraction		7.5 ± 5.8 %	20.1 ± 15.3 %	2.5 ± 2.4 %	1.7 ± 1.8 %	39.6 ± 41.5 %	28.6 ± 17.4 %
Rain	Concentration	3.8 ± 4.2	0.24 ± 0.33	0.66 ± 0.95	0.09 ± 0.13	0.05 ± 0.04	1.45 ± 1.76	1.35 ± 1.62
	Fraction		6.2 ± 8.6 %	17.2 ± 24.7 %	2.3 ± 3.4 %	1.2 ± 1.0 %	37.9 ± 45.8 %	35.2 ± 42.2 %
Entire	Concentration	11.7 ± 10.8	0.93 ± 0.88	2.34 ± 2.25	0.38 ± 0.43	0.18 ± 0.23	4.48 ± 5.91	3.42 ± 2.82
	Fraction		7.9 ± 7.5 %	19.9 ± 19.2 %	3.2 ± 3.7 %	1.5 ± 2.0 %	38.2 ± 50.4 %	29.2 ± 24.0 %

used in this study were 1.1 for nitrate, 1.2 for sulfate, 1.3 for chloride and 1.4 for organics. A RIE of 3.85 for ammonium was determined based on calibration using pure NH_4NO_3 particles.

The V-mode data were analysed to determine the mass concentrations and size distributions of the species, whereas the W-mode mass spectra were used to compute the elemental ratios (i.e. oxygen-to-carbon (O/C), hydrogen-to-carbon (H/C), nitrogen-to-carbon (N/C) and sulfur-to-carbon (S/C)) and the organic mass-to-carbon ratio (OM/OC) of the organics.[52] The high-resolution mass spectra of organics were further analysed by positive matrix factorisation (PMF)[40,56,57] to distinguish the source types of OA. Three POA factors, including a hydrocarbon-like OA (HOA) associated with traffic emissions, a cooking-influenced OA (COA), a biomass burning OA (BBOA) associated with residential wood combustion and an oxygenated OA (OOA) representing secondary OA were identified. Details on OA factor analysis and interpretation are presented by X. L. Ge, A. Setyan, Y. Sun and Q. Zhang (unpubl. data).

The hourly meteorological data including RH, temperature, rainfall, photosynthetically active radiation (PAR) and horizontal wind speed and direction during the campaign were downloaded from the California Air Resource Board (CARB) meteorological database (http://www.arb.ca.gov/aqmis2/metselect.php, accessed 3 June 2012). Concentrations of the gas pollutants (CO and ozone) were also acquired from the CARB website (http://www.arb.ca.gov/html/ds.htm, accessed 3 June 2012). Liquid water contents in the air were measured for the first week of the campaign by Herckes's group at the Arizona State University. The time reported in this paper refers to Pacific Standard Time (PST), which is the same as the local time.

Results and discussion

Overview of aerosol characteristics

Fig. 3 presents an overview of the temporal variations of the meteorological conditions, concentrations of gas pollutants (CO and O_3) and concentrations and fractions of the NR-PM_1 species

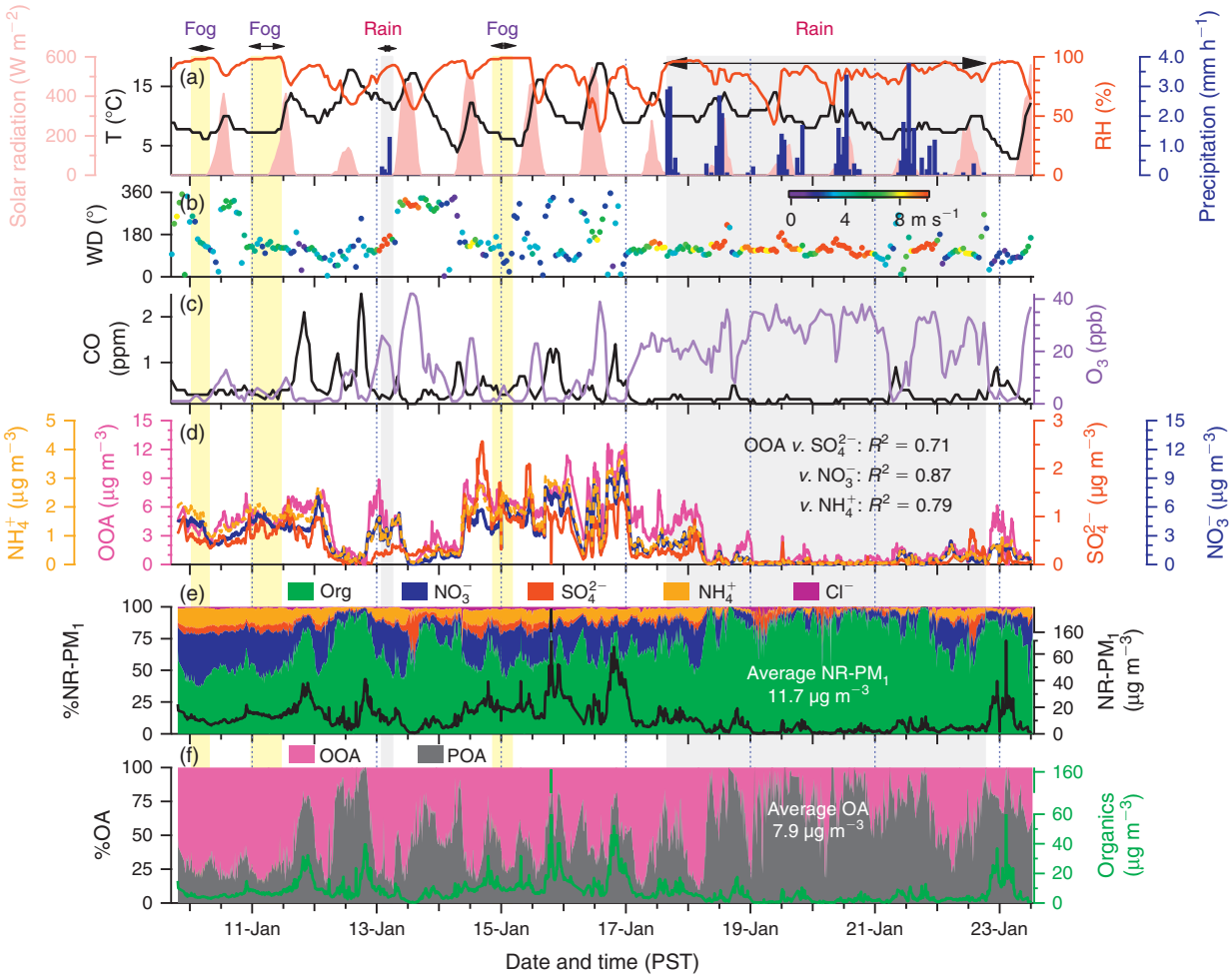

Fig. 3. Time series of (a) air temperature (T), solar radiation, relative humidity (RH) and precipitation, (b) wind direction (WD) coloured by wind speed, (c) concentrations of gas pollutants (CO and O_3), (d) mass concentrations of ammonium, OOA, sulfate and nitrate, (e) mass concentrations of total non-refractory submicrometre particles (NR-PM_1) (right *y*-axis) and the fractional contributions of organics, nitrate, sulfate, ammonium and chloride to the NR-PM_1 mass and (f) mass concentrations of organics (right *y*-axis) and the contributions of primary organic aerosol (POA) (sum of hydrocarbon-like, cooking-related and biomass burning organic aerosol) and oxygenated organic aerosol (OOA) to the total organic aerosol (OA) mass. The fog periods are identified based on high liquid water content in the air (>20 mg m^{-3}). The fog and rain periods are marked in yellow and grey, whereas periods not classified as these two types are referred to as 'other'. (PST, Pacific Standard Time.)

over the course of the study. The weather during this campaign was generally wet (average RH = 85 %) and cool (average temperature = 9.8 °C) with occasional sunshine (Fig. 3a). The diurnal variations of both RH and temperature were fairly weak, on average changing 4 °C and ~10 % between day and night (Fig. S1a, b of the Supplementary material, see http://www.publish.csiro.au/?act=view_file&file_id=EN11168_AC.pdf). The cool and humid weather is typical in the SJV during wintertime, favourable for the formation of dense and widespread radiation fogs.[5] During this study, three fog events, each lasting 7–11 h, occurred during the first week (9–15 January). The fog periods were identified based on measurements of high liquid water contents in the air (>20 mg m^{-3}; P. Herckes, ASU, pers. comm.). Consistently, the hourly RH values were always above 97 % during these periods (Fig. 3a). The first two fog events both started at ~2400 hours (0040 and 2345 hours) and persisted until a few hours after sunrise (~0700 hours). The third fog episode began earlier at night (2055 hours) and dissipated before sunrise (0405 hours). In the last week of this study, from the late afternoon of 17 January until the end of 22 January, the weather in Fresno shifted to a pattern of frequent rainfall under prevailing overcast sky conditions. A rain event that lasted for ~4 h also happened in the early morning of 13 January (Fig. 3a). The whole HR-ToF-AMS measurement can be partitioned into three conditions: foggy, rainy, and 'other'; the 'other' periods refer to those outside of the identified 'fog' and 'rain' periods mentioned above. The wind direction during this study was predominantly from the east and south-east (Fig. S1c–f). The concentrations of CO presented some large spikes in the first week, but remained at a relatively low level during the second week, during which the weather was rainy and with strong easterly winds (Fig. 3a–c). In contrast, the ozone concentrations were lower during the first week (Fig. 3c).

The concentrations of all PM_1 species varied dynamically during this study, showing very low levels (<0.4 µg m^{-3}) during rains and short excursions to high levels (>40 µg m^{-3}) associated with plumes enriched in primary organic species (Fig. 3d–f). On average, the mass concentration of total NR-PM_1 (organics + sulfate + nitrate + ammonium + chloride) was 11.7 µg m^{-3}, dominated by organics (~67 %) and nitrate (~20 %). Sulfate (average ± 1σ = 3.3 ± 3.7 %) and chloride (average ± 1σ = 1.5 ± 1.9 %) were always small contributors

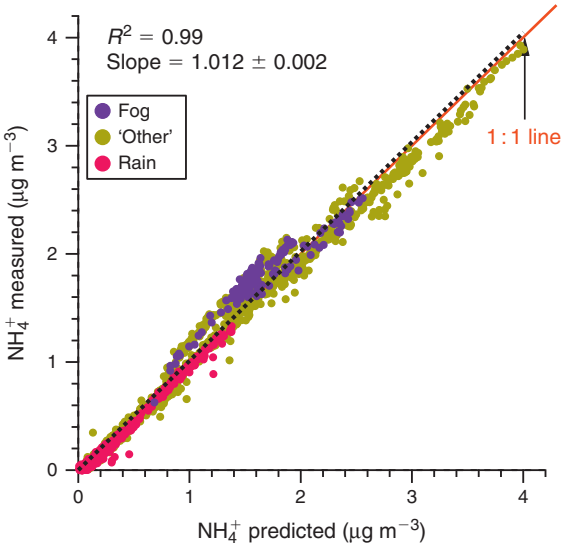

Fig. 4. Scatter plot that compares measured NH_4^+ *v.* predicted NH_4^+ concentrations. The predicted values were calculated assuming full neutralisation of the anions – sulfate, nitrate and chloride, i.e. NH_4^+ predicted = $18 \times (2 \times SO_4^{2-}/96 + NO_3^-/62 + Cl^-/35.5)$.[87] The data points are classified into fog, rain and 'other' periods as marked in Fig. 3.

to the NR-PM_1 mass. Compared to the average $PM_{2.5}$ mass of 48.3 μg m^{-3} in winter 2001–2002 reported in Chu et al.,[58] the relatively low PM_1 loading observed in this study was likely due to the strong scavenging and dilution influences from rain events (see section 'Effects of fog processing and rain scavenging on submicrometre aerosols') and possibly the lack of detection of supermicrometre particles by the AMS.

Throughout this study, nitrate, sulfate and chloride in PM_1 appeared to be fully neutralised by ammonium, i.e. the molar equivalent ratios of these anions and ammonium were near 1 (Fig. 4), indicating that the inorganic species were mainly present in the forms of NH_4NO_3, $(NH_4)_2SO_4$ and NH_4Cl. However, the average measured-to-predicted NH_4^+ ratios in PM_1 were larger than 1 during the fog episodes (Fig. 4) and the average values were 1.17 and 1.10 during the first two events. One reason for this apparent 'excess' ammonium in PM_1 was that carboxylate ions (e.g. formate, acetate and oxalate) were not accounted for in the ion-balance calculation. Enhanced dissolution of gaseous ammonia, which is abundant in Fresno, into deliquesced particles was also a possible reason. Although drying of particles in the sampling line (due to higher indoor temperature compared to ambient) would have led to evaporation of some dissolved ammonia, the drying was relatively fast (a few seconds) and some ammonia could still remain in the particle phase (A. Wexler, UC Davis, pers. comm.). In addition, when the gas and particles go through the critical orifice that lowers the pressure before the aerodynamic lens in the HR-ToF-AMS, the air cools substantially because of the isentropic expansion, allowing the re-condensation of ammonia.[59] Consistently, previous studies indeed observed that the SJV fog waters were usually alkaline[14,60] and enriched in small organic acids[14] and that the formation of ammonium nitrate in the SJV is limited by the availability of nitric acid, rather than ammonium.[61]

Previous $PM_{2.5}$ measurements in Fresno also observed the dominance of organics followed by ammonium nitrate.[58,62,63] In this study, we observed the dominance of OA (67 % of NR-PM_1 mass *v.* 20 % by nitrate) in Fresno, out of which ~57 % was contributed by POA emitted from local anthropogenic sources, including cooking, vehicle operations and residential wood combustion (Ge et al., unpubl. data). As shown in Fig. 5a, POA displayed a distinct diurnal pattern, reaching a maximum during early evening, corresponding to a period of time when emissions from rush-hour traffic, dinner cooking and residential wood burning for heating were exacerbated by collapsing boundary layer height. Similar observations were reported in Chow et al.[64] for $PM_{2.5}$.

The diurnal profiles of the concentrations of major secondary aerosol species (ammonium, nitrate, sulfate and OOA) for the entire study were generally flat (Fig. 5a), indicating the regional characteristics of these species.[50,65] These species, however, showed slightly higher concentrations during the night, likely due to enhanced gas-to-particle partitioning and aqueous-phase processing facilitated by the relatively lower temperature and higher RH at night and the frequent occurrence of night-time fogs. Lower mixed layer depth and calm wind at night may contribute to the accumulation of these species as well. The size distributions of all the secondary species showed the prevalence of a droplet accumulation mode (D_{va} of 200–700 nm) that stayed fairly constant in intensity and mode size between day and night (Fig. 5d–f). However, the size distributions of nitrate and OOA were generally broader than that of sulfate, likely due to stronger influences from gas-to-particle partitioning on the formation of these two species. The campaign-averaged size distribution of OOA was the broadest among all secondary species (Fig. 6a). The narrowest size distribution of sulfate (Fig. 6a) among all species suggests that the formation of sulfate was likely more controlled by aqueous-phase reactions during this study. This conclusion is consistent with the fact that gas-phase photochemical production of sulfate was unlikely an important process given the overall low solar irradiation combined with the low SO_2 concentration in the region. Aqueous-phase reactions, which are a well known pathway for sulfate formation in the atmosphere,[66] were likely important in Fresno during winter because of the overall wet and foggy conditions.

The POA concentration increased substantially at night (Fig. 5a) and was associated with a broadening of the size distribution down to $D_{va} < 100$ nm (Fig. 5c). The particle number distribution also indicated enhanced emissions of ultrafine particles at night (Fig. 5b). The average size distribution of total POA (Fig. 6a) was clearly different than those of secondary species, showing a bimodal distribution with a more prominent mode at ~150 nm that reflects the influences from primary emissions. As a result, POA dominated the composition of ultrafine particles whereas the contributions of secondary species (OOA + sulfate + nitrate + chloride + ammonium) gradually increased with the increase of particle sizes (Fig. 6b). Overall, POA accounted for more than 90 % of the mass in ultrafine particles and secondary species accounted for more than 75 % of the mass in accumulation mode particles.

Effects of fog processing and rain scavenging on submicrometre aerosols

As shown in Figs 3 and S1c, winds readily blew from a narrow angle between eastern and south-eastern directions over the course of the campaign. Although the wind speed was generally low during the fog periods, much stronger winds were often encountered during precipitation (Fig. S1c–f). This wind pattern

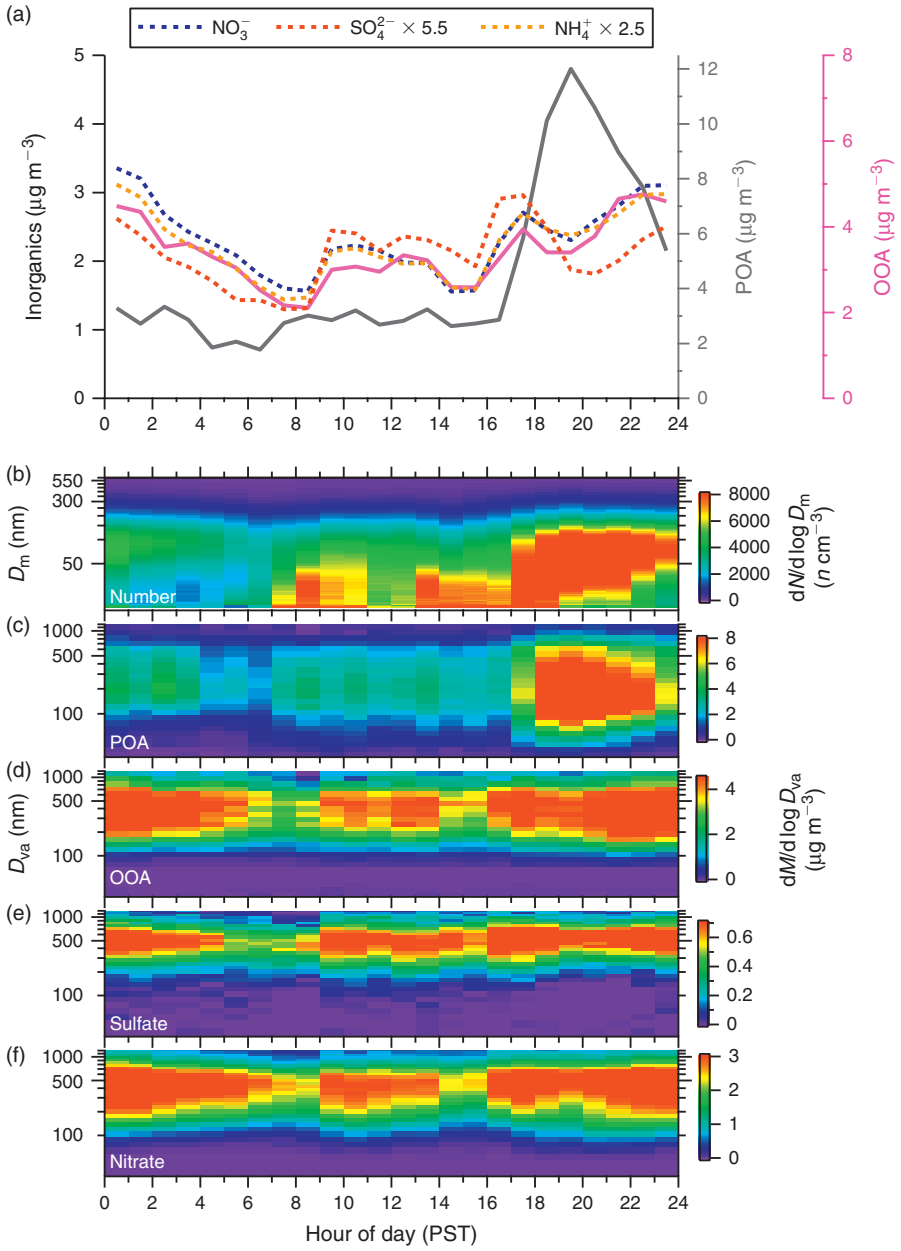

Fig. 5. Diurnal profiles of (a) inorganic species (sulfate, nitrate, and ammonium, left *y*-axis), primary organic aerosol (POA) and oxygenated organic aerosol (OOA), (b) particle number distributions recorded by the SMPS, and (c–f) mass-based size distributions of POA, OOA, sulfate and nitrate. (PST, Pacific Standard Time; D_{va}, vacuum aerodynamic diameter; D_m, mobility diameter.)

indicates small variations in terms of particle sources, which provides a reasonable Eulerian frame of reference allowing us to investigate the evolution of ambient aerosols under different conditions. Specifically, aerosols were exposed to highly humid conditions during both fog and rain periods (Fig. 3a). However, given that raindrops (~1 mm) are much larger than fog droplets (mean diameter of ~10–15 μm), wet scavenging of aerosols is much more effective in the rain.

To investigate the effects of fogs and rains on aerosol characteristics, we compared the average concentrations and size distributions of individual species between the three weather conditions: foggy, rainy and other. As all three fog episodes occurred within the time window between 2100 and 1100 hours of the 2nd day, we show in Figs 7 and 8 the comparisons using data sampled during this time period only. The results corresponding to the entire periods defined in Fig. 3 are overall similar to those determined for the period from 2100 to 1100 hours only (Figs S3, S4). In the rest of this manuscript, our discussions on the comparisons refer to the results corresponding only to the period from 2100 to 1100 hours, unless otherwise noted. The average NR-PM_1 mass loading was lower during both foggy (14.2 μg m^{-3}) and rainy days (3.8 μg m^{-3}) than during 'other' periods (15.3 μg m^{-3}; Table 1). In particular, the occurrence of rains reduced the NR-PM_1 mass concentration by more than a factor of 3 (Fig. 7). Aerosol compositions were very different among these three conditions too. Compared to the 'other' periods, the average concentrations of ammonium sulfate, ammonium nitrate and OOA all increased

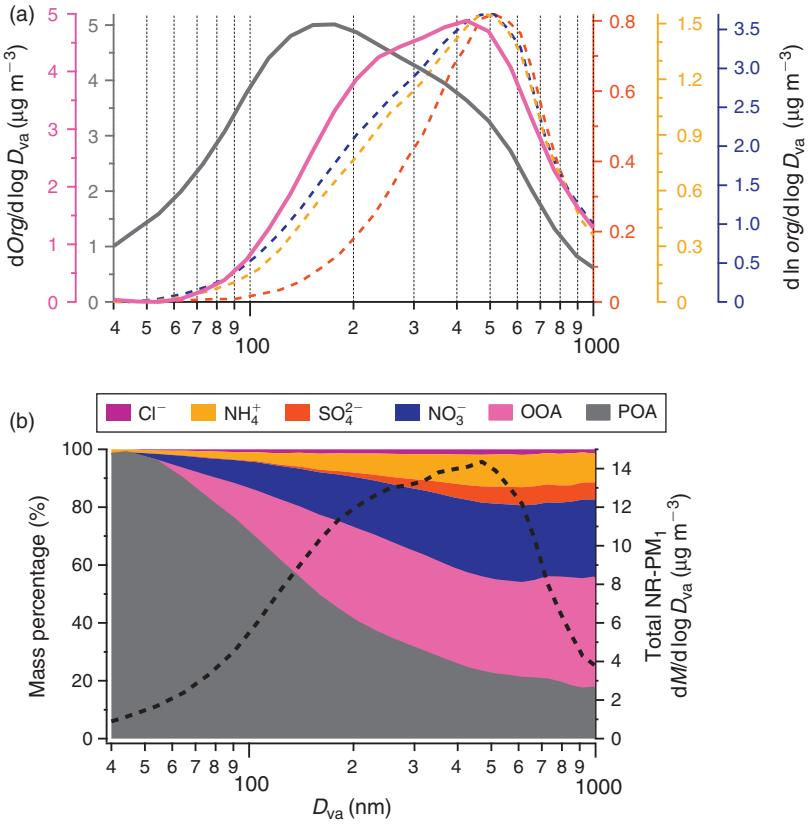

Fig. 6. Average size distributions of (a) the mass concentrations of individual non-refractory submicrometre particles (NR-PM_1) species, and (b) total NR-PM_1 mass (right *y*-axis) and the fractions of individual species (left *y*-axis) for the entire campaign. (D_{va}, vacuum aerodynamic diameter; POA, primary organic aerosol; OOA, oxygenated organic aerosol.)

during fogs whereas that of POA decreased (Fig. 7a and Table 1). The decrease of POA during fog episodes was mainly attributed to reduced primary emissions from traffic, food cooking and residential wood burning from midnight to early morning. The total concentration of OOA, sulfate, nitrate and ammonium increased by an average 3.0 μg m^{-3} during fog periods compared to 'other' periods (Fig. 7a), indicating that secondary aerosol production outweighed wet scavenging in fogs. As a result, the mass fraction of secondary species was the highest (85 % of NR-PM_1) during fog periods (Fig. 7b and Table 1). In contrast, POA accounted for a large fraction (~40 %) of NR-PM_1 mass during rainy days (Fig. 7b and Table 1), resulting from preferential wet scavenging of more hygroscopic secondary aerosol species and constant inputs of POA from local emissions. Similar observations were made in New York City based on a detailed case study of size-resolved aerosol concentration and composition during a wet-scavenging event.[67]

Among the three conditions, the average size distributions of all species, including sulfate, nitrate, OOA and POA, were the narrowest during fogs, and were associated with an enhancement in the accumulation mode peaking at ~500 nm in D_{va} (Fig. 8). Particles with mass median aerodynamic diameters of ~0.4–1 μm are usually referred to as droplet mode because they are primarily formed from aqueous-phase reactions in clouds and wet aerosols.[68–71] In contrast, gas-to-particle partitioning of secondary species formed from gas-phase reactions mostly modifies the condensation mode (<0.2 μm) particles.[66,69] This is because the condensational growth rate of a particle decreases with the increase of size, therefore, in the typical atmospheric lifetime of particles, the condensation mode does not grow beyond 0.2 μm.[70] Note that D_{va} (the aerodynamic diameter measured in the free-molecular regime) is different than the classical aerodynamic diameter measured in the continuum regime (D_{ca}) in that D_{va} equals D_{ca} times the square root of particle density for spherical particles but they relate differently to the dynamic shape factor.[54] Because the average density of particles was ~1.3 g cm^{-3} in this study and particles dominated by secondary species were likely to be spherical, the D_{va}/D_{ca} ratio was expected to be close to 1. In addition, the droplet modes defined in Hering and Friedlander[68] and in John et al.[69] were based on size measurements under low pressure; the reported particle diameters were thus similar to D_{va}. The significant mass increases of sulfate, nitrate and OOA in the droplet mode during fog episodes (Fig. 8a–c) are thus consistent with aqueous-phase production of these species led by fog processing. The narrowing of the size distribution of POA (Fig. 8d) during fog events was probably due to coagulation or due to the mass production of secondary species which appear to be internally mixed with POA during fogs.

In contrast, the size distributions of sulfate, nitrate and OOA were much broader during rain periods (Fig. 8a–c) in association with huge reductions of the mass concentrations (Fig. 7a and Table 1). This observation reflects the effects of rain on aerosol chemistry and microphysics, which are governed by wet scavenging that preferentially removes hygroscopic secondary species enriched in the droplet mode. However, the fact that these secondary species all demonstrate a broader size

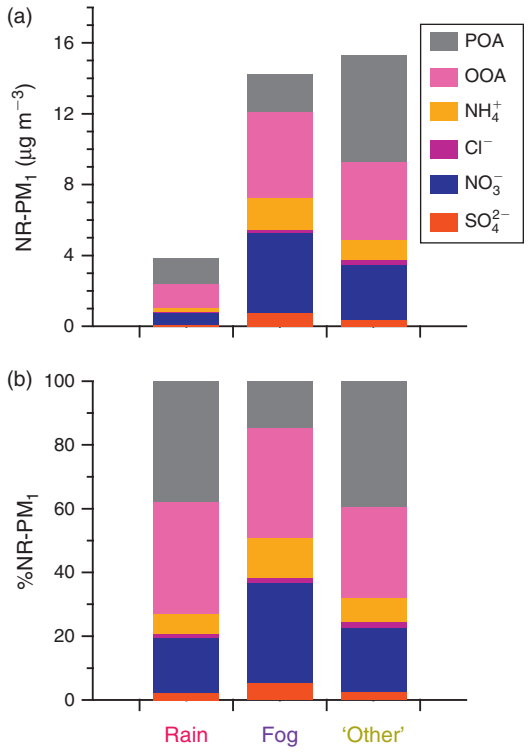

Fig. 7. (a) Average mass concentrations and (b) fractional contributions of aerosol species to the total non-refractory submicrometre particles ($NR\text{-}PM_1$) mass measured from 2100 hours at night until 1100 hours in the morning of the 2nd day during the fog, 'other', and rain periods as marked in Fig. 3. (POA, primary organic aerosol; OOA, oxygenated organic aerosol.)

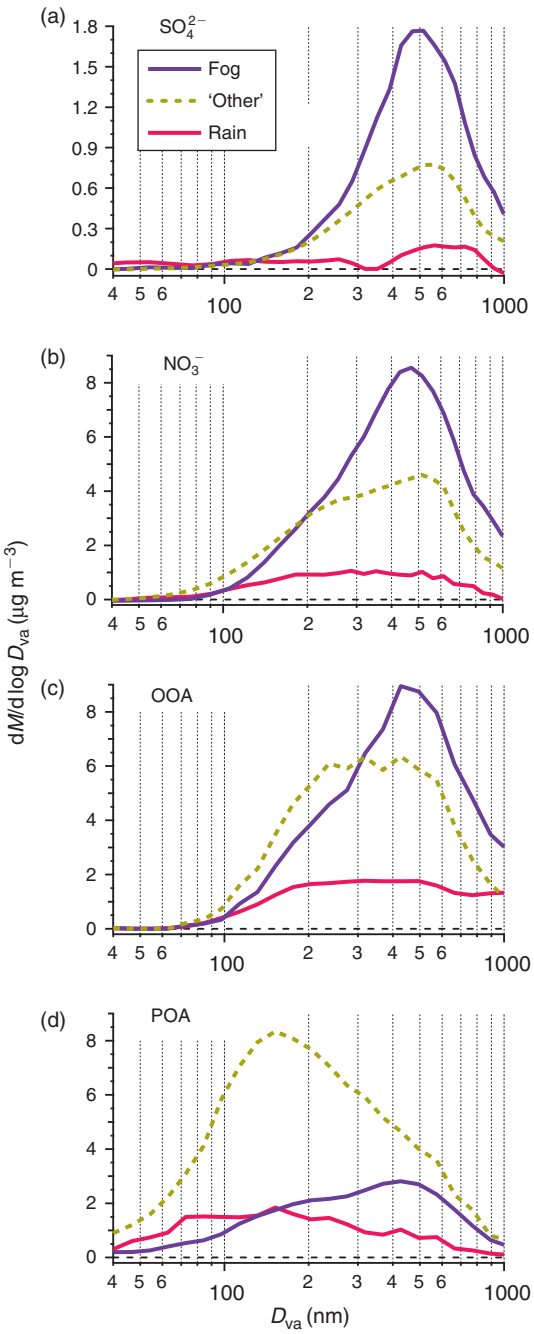

Fig. 8. Averaged mass-based size distributions of (a) sulfate, (b) nitrate, (c) oxygenated organic aerosol (OOA) and (d) primary organic aerosol (POA) from 2100 hours at night until 1100 hours in the morning of the 2nd day during the fog, 'other', and rain periods as marked in Fig. 3. (D_{va}, vacuum aerodynamic diameter.)

distribution with a relatively enhanced condensation mode peaking at ~200 nm (D_{va}) during rains compared to no-rain periods also suggests that condensational growth of secondary aerosol species might have occurred due to the continuous emissions of both primary particles and gaseous species. This assumption is consistent with the observation that primary ultrafine particles from combustion sources dominated aerosol population during the rain periods (Figs 3f, S2). However, because rains were usually accompanied by strong winds (Fig. 3b), air pollutants were much diluted and the concentrations of primary pollutants such as POA and CO were on average lower during rain periods compared to the 'other' conditions (Figs 3, 7).

Effects of aqueous-phase processing on SOA formation

As discussed above, raindrops had significant scavenging effects on aerosol whereas fog processing enhanced the production of secondary aerosol species (Figs 7, 8). Because the increases of sulfate, nitrate and OOA all occurred in the submicrometre droplet mode (Fig. 8), aqueous-phase chemistry seems to have played an important role. An explanation is that under the very high RH condition in fogs, water-rich particles as well as fog droplets are able to capture more soluble gases such as ammonia, nitric acid, NO_x and SO_2, leading to more efficient production of ammonium nitrate and sulfate. Similarly, the dissolution of water-soluble volatile organic compounds (VOCs) may also be enhanced in fog drops and deliquesced particles and the aqueous-phase reactions of these compounds may generate low volatility species that remain in the particle phases after water evaporates.[66,72] This SOA formation pathway in aerosol water was supported by both laboratory studies[73,74] and field observations.[41]

Compared to the 'other' periods, the concentration of OOA increased by an average of ~0.5 μg m^{-3} during fog episodes (Fig. 7a, Table 1), and the increase occurred primarily in the droplet mode whereas OOA concentration in particles smaller than 300 nm (D_{va}) actually decreased (Fig. 8c). Because fog droplets, which are too big to be transmitted by the AMS aerodynamic lens, could have scavenged a fraction of the submicrometre aerosols, we analysed the fog waters sampled

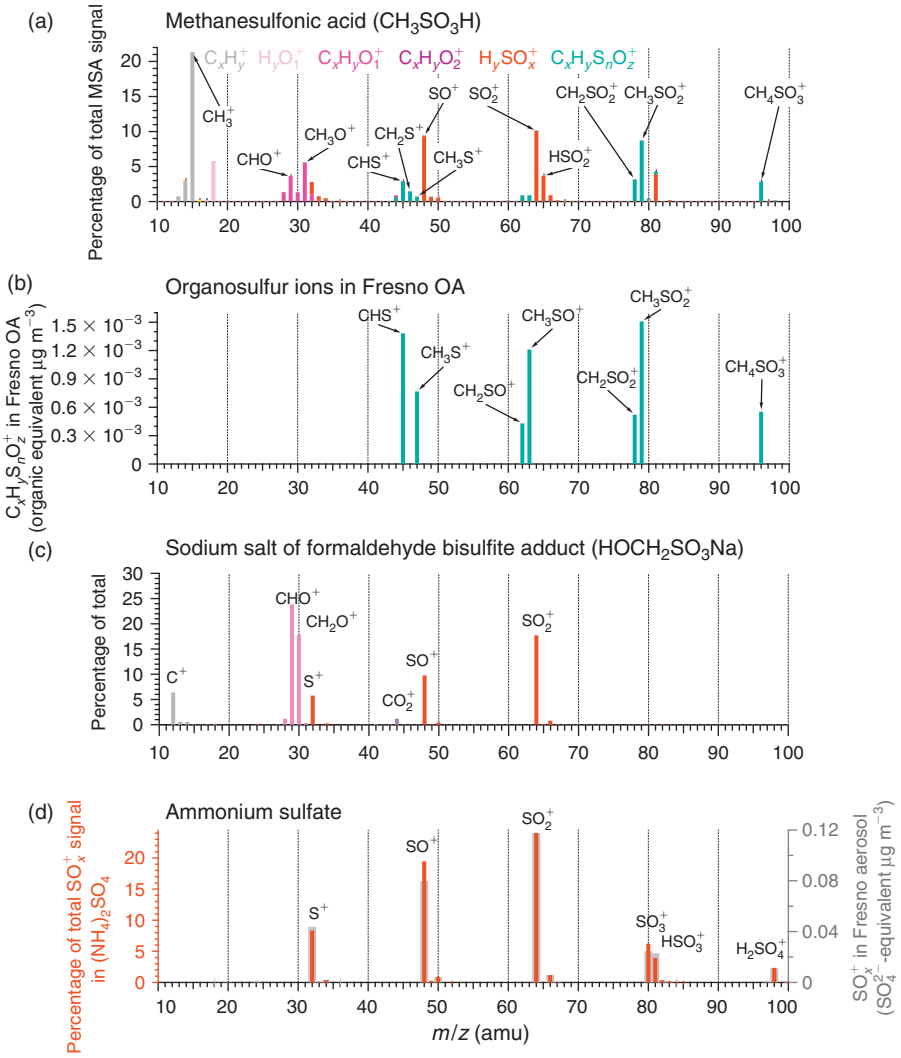

Fig. 9. High-resolution aerosol mass spectrometer (HR-AMS) spectra of (a) methanesulfonic acid (MSA, CH_3SO_3H), (b) average signals of the organosulfur ions detected in Fresno OA, (c) sodium hydroxymethanesulfonate ($HOCH_2SO_3Na$) and (d) ammonium sulfate and the average sulfate signals detected in ambient Fresno aerosol. Note water and ammonium ions are excluded in (d).

during the three fog episodes in the laboratory using the HR-ToF-AMS based on the method reported in Sun et al.[75] We found that the composition of fog water organics was almost identical to that of OOA indicating that OOA was preferentially scavenged compared to POA. The total amount of OOA in fog waters and interstitial aerosols during fog events exceeded the average OOA concentration of the 'other' period by ~1.9 µg m^{-3}, corroborating aqueous-phase SOA formation. An increase of SOA concentrations was observed recently during winter fog episodes in Kanpur, India.[76] In addition, aqueous-phase SOA production was observed based on single particle mass spectrometry in a fog event in London although the OOA concentration determined by an AMS did not show an increase,[41] consistent with our observation that a portion of the OOA was incorporated into fog droplets.

Additional evidence for aqueous-phase SOA production during this study is the detection of methanesulfonic acid (MSA, CH_3SO_3H) or mesylate ($CH_3SO_3^-$, the deprotonated anion of MSA) in PM_1. In the HR-ToF-AMS data, several sulfur-containing organic ions (i.e. $C_xH_yS_nO_z^+$, in which $x \geq 1$, $y \geq 1$, $n \geq 1$, $z \geq 0$) were observed (Fig. 9b). Among them, $CH_2SO_2^+$, $CH_3SO_2^+$ and $CH_4SO_3^+$ were separated well from adjacent ions (see Fig. S5e–g) and thus quantified with high confidence. The correlations among the time series of $CH_2SO_2^+$, $CH_3SO_2^+$ and $CH_4SO_3^+$ were tight (Fig. S6) and the signal intensity ratios were remarkably similar to those observed in the pure MSA spectrum acquired by the HR-ToF-AMS (Fig. 9a, b), confirming the presence MSA or mesylate in Fresno aerosols. The other $C_xH_yS_nO_z^+$ ions detected (i.e. CHS^+, CH_3S^+ CH_2SO^+ and CH_3SO^+; Fig. 9b) were likely contributed by other organosulfur compounds in addition to MSA, because (1) they correlated poorly with each other or with $CH_2SO_2^+$, $CH_3SO_2^+$ and $CH_4SO_3^+$ and (2) their signal ratios in ambient aerosols were clearly different than those observed in MSA (Fig. 9a, b). However, it is important to point out that the quantifications of CHS^+, CH_3S^+ CH_2SO^+ and CH_3SO^+ were also subjected to interferences from adjacent ions (Fig. S5a–d). Given that $CH_2SO_2^+$, $CH_3SO_2^+$ and $CH_4SO_3^+$ appear to be the signature ions of MSA, we estimated the MSA concentrations (mMSA) using the following equation:

$$m\mathrm{MSA} = (m\mathrm{CH_2SO_2^+} + m\mathrm{CH_3SO_2^+} + m\mathrm{CH_4SO_3^+})/0.147 \quad (1)$$

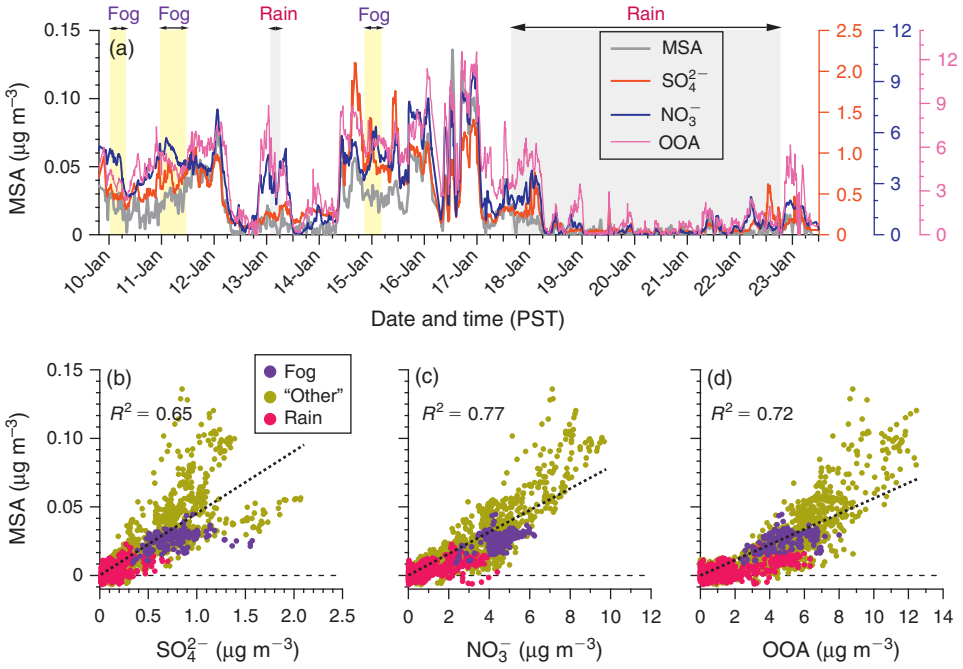

Fig. 10. (a) Time series of methanesulfonic acid (MSA), sulfate, nitrate and oxygenated organic aerosol (OOA), and scatter plots of MSA *v.* (b) sulfate, (c) nitrate and (d) OOA. The data points are classified into fog, rain and 'other' periods as marked in Fig. 3. (PST, Pacific Standard Time.)

where $m\mathrm{CH_2SO_2^+}$, $m\mathrm{CH_3SO_2^+}$ and $m\mathrm{CH_4SO_3^+}$ are the signal intensities of these three ions measured in ambient aerosols (organic-equivalent μg m^{-3}) and 0.147 is their fractional contribution to the total signal in the HR-ToF-AMS spectrum of pure MSA (Fig. 9a). Note that the MSA spectrum acquired in this study shows a very similar pattern to that of the HR MSA spectrum reported in Zorn et al.[77] The average concentration of MSA during this study was estimated at 0.018 μg m^{-3}, which corresponded to ~0.5 % of the OOA mass.

Previous studies indicate that MSA is a SOA species that mainly originates from the oxidation of dimethyl sulfide (DMS) emitted from oceans.[78] This conclusion was also supported by recent measurements with highly time-resolved aerosol mass spectrometry. For example, Phinney et al.[79] and Zorn et al.[77] quantified MSA over sea using AMS and found that the diurnal trends of particulate MSA concentration correlated with oceanic biological activities. In addition, using a laser-based single-particle mass spectrometer, Gatson et al.[80] and Huffman et al.[81] detected MSA in particles in Riverside, an inland urban site in southern California. Gatson et al.[80] found that the highest ambient MSA concentrations were associated with daily westerly winds that delivered coastal emissions across the Los Angeles (LA) Basin to Riverside, and also demonstrated that the production of MSA was due to blooms of DMS-producing organisms along the Californian coast. In this study, however, particulate MSA does not seem to show a clear association with emissions from the ocean. The Pacific Ocean is ~160 miles (~257 km) to the west of Fresno but winds blew from the east and south-east for most of the time during this study (Figs 3b, S1c), indicating that the MSA observed in Fresno was likely associated with non-oceanic sources. Indeed, widespread continental sources for DMS and dimethyl sulfoxide (DMSO), both of which are precursors of MSA, were observed previously.[82,83]

As shown in Fig. 10, MSA correlated well with sulfate, nitrate and OOA (R^2 = 0.65, 0.77 and 0.72), suggesting that the secondary aerosol species shared common oxidation pathways. Because sulfate was likely produced mainly by aqueous-phase reactions in this study (see section 'Overview of aerosol characteristics'), the good correlations further suggest important roles of aqueous-phase processes on the formation of nitrate, OOA and MSA. Previous studies indeed found that the formation of MSA can be strongly enhanced by aqueous-phase processing (see Barnes et al.[84] and references therein).

Hydromethanesulfonate (HMS) ($\mathrm{HOCH_2SO_3H}$), the $\mathrm{HSO_3^-}$ adduct of formaldehyde, has been identified as a tracer for aqueous-phase SOA production in fogs and clouds (see Whiteaker and Prather[85] and references therein). This compound was detected in submicrometre particles by laser ablation single particle mass spectrometry.[85,86] However, probably due to thermal decomposition on the vaporiser (kept at ~600 °C in this study), the HR-ToF-AMS spectrum of HMS is dominated by $\mathrm{CHO^+}$, $\mathrm{CH_2O^+}$, $\mathrm{SO^+}$ and $\mathrm{SO_2^+}$ (Fig. 9c), which are the common ion fragments in ambient aerosols. No characteristic AMS ions suitable for fingerprinting HMS were identified. However, unlike ammonium sulfate (Fig. 9d), HMS doesn't generate $\mathrm{SO_3^+}$, $\mathrm{HSO_3^+}$ or $\mathrm{H_2SO_4^+}$ ions in the HR-ToF-MS (Fig. 9c). We thus expect to see increases in the peak ratios of $\mathrm{SO^+/SO_3^+}$, $\mathrm{SO^+/HSO_3^+}$, $\mathrm{SO^+/H_2SO_4^+}$, $\mathrm{SO_2^+/SO_3^+}$, $\mathrm{SO_2^+/HSO_3^+}$ and $\mathrm{SO_2^+/H_2SO_4^+}$ in ambient aerosols should a significant amount of HMS coexist with sulfate. Yet, such increases were not observed, suggesting that HMS may not be produced in an appreciable amount in aerosols during this study. A possible reason is the very low $\mathrm{SO_2}$ concentrations in the region leading to a low $\mathrm{HSO_3^-}$ concentration in fog droplets. Nevertheless, the observation of significant quantities of sulfur-containing organic ions and the detection of MSA that closely correlate with major secondary aerosols species suggests that aqueous-phase reactions, enhanced by frequent fog episodes, may have

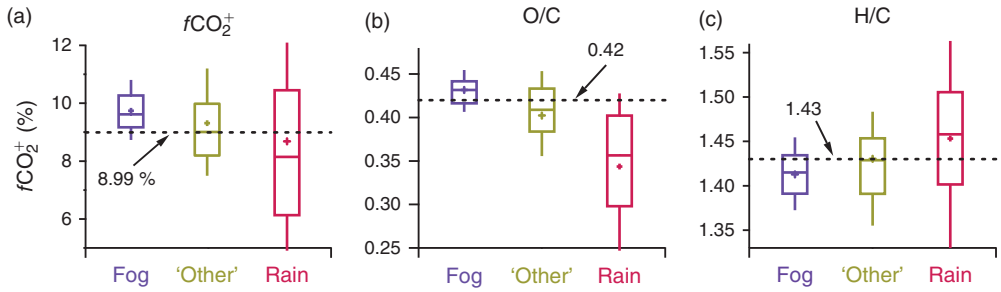

Fig. 11. Variations of (a) fCO_2^+ (fraction of CO_2^+ signal in the organic mass spectrum), and the elemental ratios of (b) O/C and (c) H/C in the oxygenated organic aerosol plus residual factor (OOA_{resid}) during fog, 'other' and rain periods as marked in Fig. 3. The whiskers above and below the boxes are the 90th and 10th percentiles; the upper and lower boundaries of the boxes indicate the 75th and 25th percentiles; the lines and the markers inside the boxes are the median and mean values. The dashed lines indicate the corresponding values of the oxygenated organic aerosol (OOA) factor from positive matrix factorisation (PMF).

played an important role in SOA production in the SJV region during winter.

Although both gaseous and aqueous-phase reactions are likely important sources of SOA in Fresno during winter, we were able to separate out only one OOA factor for this study. A possible explanation is that the bulk compositions of SOA produced from these two reaction pathways are overall similar, so that their mass spectra are not different enough to be separated by factor analysis. Another possible reason is that ambient particles in Fresno during wintertime were subjected to convoluted gas-phase and aqueous-phase reactions and aerosol populations are thus indistinguishable according to individual processes. As a result, the one OOA factor identified by the PMF model in this study likely consisted of SOA species formed from both gas-phase and aqueous-phase reactions.

Because every factor extracted by PMF is assumed to have a constant spectrum throughout a study period, the chemical variations of the factors would be represented in the residuals of the model fit defined as the differences between the measured signals and the reconstructed signals.[40] To examine the chemical variations in OOA, we determined an $\mathbf{OOA_{resid}}$ matrix by subtracting the contributions of HOA, COA and BBOA from the measured OA mass spectrometric matrix (**ORG**):

$$\mathbf{OOA_{resid}} = \mathbf{ORG} - (\mathbf{ts_{HOA}} \times \mathbf{ms_{HOA}} + \mathbf{ts_{COA}} \times \mathbf{ms_{COA}} + \mathbf{ts_{BBOA}} \times \mathbf{ms_{BBOA}})$$

where $\mathbf{ts_{HOA}}$, $\mathbf{ts_{COA}}$ and $\mathbf{ts_{BBOA}}$ are column vectors representing the time series of HOA, COA and BBOA, and $\mathbf{ms_{HOA}}$, $\mathbf{ms_{COA}}$ and $\mathbf{ms_{BBOA}}$ are row vectors representing their corresponding mass spectra resolved from PMF. Note that although the mass spectra of HOA, COA and BBOA may actually vary from time to time in ambient air, we assume they are constant during the study period. Alternatively, $\mathbf{OOA_{resid}}$ equals the **OOA** matrix ($\mathbf{ts_{OOA}} \times \mathbf{ms_{OOA}}$) plus the residual matrix from the 4-factor solution. The time series of OOA_{resid}, i.e. $\mathbf{ts_{OOAresid}}$ (a column vector), was subsequently determined by summing all the elements in each row of the $\mathbf{OOA_{resid}}$ matrix.

The mass concentrations of individual elements in **OOA** and $\mathbf{OOA_{resid}}$ correlate well with a linear regression slope of ~1 and the time series of OOA_{resid} agree well with that of OOA (Fig. S7), consistent with the fact that the 4-factor solution was able to account for most variance of the **ORG** matrix. The OOA_{resid} factor, however, is different to the OOA factor directly from PMF in that the mass spectrum of OOA_{resid} is variable as a function of time whereas that of the OOA is constant. The variations in the mass spectrum of OOA_{resid} allowed us to examine the bulk chemical differences of the oxygenated species among different meteorological conditions. As shown in Fig. 11, both the fCO_2^+ (the fractional contribution of CO_2^+ to the total organic signal) and the O/C ratio of OOA_{resid} were on average higher during fogs than during the other two types of periods whereas a decrease of the average H/C ratio was observed during foggy conditions. The averaged HRMS of the OOA_{resid} for the three conditions are shown in Fig. S8. These results indicate that the oxidation degree of SOA was likely enhanced by fog processing. Similarly, previous studies observed that SOA produced in the aqueous phase is generally more oxygenated than SOA formed in the gas phase.[66]

Conclusions

We deployed a HR-ToF-AMS and a SMPS to characterise the chemical composition and size distributions of submicrometre aerosols in Fresno, CA during winter 2010. PM_1 was dominated by secondary species, including oxygenated organics (~29 %), ammonium nitrate (~26 %), ammonium sulfate (~4.4 %) and ammonium chloride (~2.3 %). Primary organic species emitted from food cooking, fossil fuel and residential wood combustions together accounted for ~38 % of the PM_1 and ~57 % of total OA. The temporal and diurnal variation profiles of sulfate, nitrate, ammonium and OOA correlated well with each other, suggesting that their formation pathways were generally similar during this study. The size distributions of all secondary species demonstrated a prevailing accumulation droplet mode (~500 nm in D_{va}), indicating strong influences from aqueous processes. POA showed a different behaviour – its concentration reached a maximum at early night and its mass-based size distribution peaked at a small mode (~150 nm in D_{va}), reflecting the influences from different emission sources (i.e. transportation, cooking and wood burning).

Fogs and rains have very different effects on aerosol properties. For instance, aerosol concentrations were substantially reduced during rains and the particles became enriched in primary organic species, indicating the predominant wet-scavenging effects of raindrops on the more hygroscopic secondary aerosol species. In contrast, all secondary aerosol species increased in concentration, and end up accounting for an average 85 % of NR-PM_1 mass, during fog periods despite scavenging by fog drops (although to a lesser degree compared to rain scavenging). This observation, combined with the substantial enhancements of the droplet mode in the size

distributions of sulfate, nitrate and OOA during fogs, indicates the production of secondary aerosols species by aqueous reactions. Further evidence for aqueous formation of SOA is the detection of mesylate ($CH_3SO_3^-$) that correlated tightly with sulfate. It is known that the atmospheric formation of both MSA and sulfate are strongly enhanced by cloud and fog processes. The aqueous-phase reaction pathway was particularly favourable for sulfate formation during this study due to high humidity and frequent fog episodes and limited gaseous oxidation associated with low solar radiation. In fact, the good correlations among all secondary species point to the general importance of aqueous-phase reactions, which could occur in both airborne droplets and aqueous particles, on secondary aerosol production in the Central Valley of California during winter. Our results also show that fog processing appeared to have increased the oxidation degree of the OOA/SOA. In summary, our study suggests that aqueous-phase processing can have important effects on submicrometre aerosol loading, chemistry and microphysics, and thus significantly alter their relevant climatic and human health effects.

Acknowledgments

This research was supported by the San Joaquin Valley Aerosol Health Effects Research Center (SAHERC) funded by the United States Environmental Protection Agency through grant RD-83241401-0 to the University of California, Davis. Although the research described in the article has been funded by the USA EPA, it has not been subjected to the Agency's required peer and policy review and therefore does not necessarily reflect the views of the Agency and no official endorsement should be inferred. Additional support for this work was provided by the Office of Science (BER), USA Department of Energy, grant number DEFG02-08ER64627, DESC0002191, the California Agricultural Experiment Station (Project CA-D-ETX-2102-H) and the UC Davis Atmospheric Aerosol Health (AAH) program. The authors thank Dr Pierre Herckes at the Arizona State University for providing liquid water content measurement data.

References

[1] S. J. Ghan, S. E. Schwartz, Aerosol properties and processes: a path from field and laboratory measurements to global climate models. *Bull. Am. Meteorol. Soc.* **2007**, *88*, 1059. doi:10.1175/BAMS-88-7-1059

[2] C. A. Pope, R. T. Burnett, M. J. Thun, E. E. Calle, D. Krewski, K. Ito, G. D. Thurston, Lung cancer, cardiopulmonary mortality, and long-term exposure to fine particulate air pollution. *JAMA* **2002**, *287*, 1132. doi:10.1001/JAMA.287.9.1132

[3] N. Mahowald, Aerosol indirect effect on biogeochemical cycles and climate. *Science* **2011**, *334*, 794. doi:10.1126/SCIENCE.1207374

[4] M. Ngo, K. Pinkerton, S. Freeland, M. Geller, W. Ham, S. Cliff, L. Hopkins, M. Kleeman, U. Kodavanti, E. Meharg, L. Plummer, J. Recendez, M. Schenker, C. Sioutas, S. Smiley-Jewell, C. Haas, J. Gutstein, A. Wexler, Airborne particles in the San Joaquin Valley may affect human health. *Cal. Ag.* **2010**, *64*, 12. doi:10.3733/CA.V064N01P12

[5] P. Herckes, H. Chang, T. Lee, J. L. Collett, Air pollution processing by radiation fogs. *Water Air Soil Pollut.* **2007**, *181*, 65. doi:10.1007/S11270-006-9276-X

[6] D. J. Jacob, F. H. Shair, J. M. Waldman, J. W. Munger, M. R. Hoffmann, Transport and oxidation of SO_2 in a stagnant foggy valley. *Atmos. Environ.* **1987**, *21*, 1305. doi:10.1016/0004-6981(67)90077-7

[7] S. N. Pandis, J. H. Seinfeld, C. Pilinis, Heterogeneous sulfate production in an urban fog. *Atmos. Environ., A Gen. Topics* **1992**, *26*, 2509. doi:10.1016/0960-1686(92)90103-R

[8] J. W. Munger, J. Collett Jr, B. C. Daube, M. R. Hoffmann, Carboxylic acids and carbonyl compounds in southern California clouds and fogs. *Tellus B Chem. Phys. Meterol.* **1989**, *41B*, 230. doi:10.1111/J.1600-0889.1989.TB00303.X

[9] X. Rao, J. L. Collett Jr, Behavior of S^{IV} and formaldehyde in a chemically heterogeneous cloud. *Environ. Sci. Technol.* **1995**, *29*, 1023. doi:10.1021/ES00004A024

[10] D. Grosjean, B. Wright, Carbonyls in urban fog, ice fog, cloudwater and rainwater. *Atmos. Environ.* **1983**, *17*, 2093. doi:10.1016/0004-6981(83)90368-2

[11] M. C. Facchini, J. Lind, G. Orsi, S. Fuzzi, Chemistry of carbonyl compounds in Po Valley fog water. *Sci. Total Environ.* **1990**, *91*, 79. doi:10.1016/0048-9697(90)90289-7

[12] D. J. Jacob, J. W. Munger, J. M. Waldman, M. R. Hoffmann, The H_2SO_4–HNO_3–NH_3 system at high humidities and in fogs 1. Spatial and temporal patterns in the San Joaquin Valley of California. *J. Geophys. Res. – Atmos.* **1986**, *91*(D1), 1073. doi:10.1029/JD091ID01P01073

[13] D. Lillis, C. N. Cruz, J. Collett Jr, L. W. Richards, S. N. Pandis, Production and removal of aerosol in a polluted fog layer: model evaluation and fog effect on PM. *Atmos. Environ.* **1999**, *33*, 4797. doi:10.1016/S1352-2310(99)00264-2

[14] J. L. Collett Jr, K. J. Hoag, D. E. Sherman, A. Bator, L. W. Richards, Spatial and temporal variations in San Joaquin Valley fog chemistry. *Atmos. Environ.* **1998**, *33*, 129. doi:10.1016/S1352-2310(98)00136-8

[15] J. L. Collett Jr, A. Bator, D. E. Sherman, K. F. Moore, K. J. Hoag, B. B. Demoz, X. Rao, J. E. Reilly, The chemical composition of fogs and intercepted clouds in the United States. *Atmos. Res.* **2002**, *64*, 29. doi:10.1016/S0169-8095(02)00077-7

[16] C. Anastasio, B. C. Faust, C. J. Rao, Aromatic carbonyl compounds as aqueous-phase photochemical sources of hydrogen peroxide in acidic sulfate aerosols, fogs, and clouds. 1. Non-phenolic methoxybenzaldehydes and methoxyacetophenones with reductants (phenols). *Environ. Sci. Technol.* **1997**, *31*, 218. doi:10.1021/ES960359G

[17] S. Raja, R. Raghunathan, X. Y. Yu, T. Y. Lee, J. Chen, R. R. Kommalapati, K. Murugesan, X. Shen, Y. Qingzhong, K. T. Valsaraj, J. L. Collett Jr, Fog chemistry in the Texas–Louisiana gulf coast corridor. *Atmos. Environ.* **2008**, *42*, 2048. doi:10.1016/J.ATMOSENV.2007.12.004

[18] M. A. J. Harrison, S. Barra, D. Borghesi, D. Vione, C. Arsene, R. Iulian Olariu, Nitrated phenols in the atmosphere: a review. *Atmos. Environ.* **2005**, *39*, 231. doi:10.1016/J.ATMOSENV.2004.09.044

[19] W. Winiwarter, H. Fierlinger, H. Puxbaum, M. C. Facchini, B. G. Arends, S. Fuzzi, D. Schell, U. Kaminski, S. Pahl, T. Schneider, A. Berner, I. Solly, C. Kruisz, Henry's law and the behavior of weak acids and bases in fog and cloud. *J. Atmos. Chem.* **1994**, *19*, 173. doi:10.1007/BF00696588

[20] S. Decesari, M. C. Facchini, S. Fuzzi, E. Tagliavini, Characterization of water-soluble organic compounds in atmospheric aerosol: a new approach. *J. Geophys. Res. – Atmos.* **2000**, *105*(D1), 1481. doi:10.1029/1999JD900950

[21] Q. Zhang, C. Anastasio, Chemistry of fog waters in California's Central Valley – Part 3. Concentrations and speciation of organic and inorganic nitrogen. *Atmos. Environ.* **2001**, *35*, 5629. doi:10.1016/S1352-2310(01)00337-5

[22] Q. Zhang, C. Anastasio, Conversion of fogwater and aerosol organic nitrogen to ammonium, nitrate, and NO_x during exposure to simulated sunlight and ozone. *Environ. Sci. Technol.* **2003**, *37*, 3522. doi:10.1021/ES034114X

[23] J. W. Hutchings, B. Ervens, D. Straub, P. Herckes, *N*-nitrosodimethylamine occurrence, formation and cycling in clouds and fogs. *Environ. Sci. Technol.* **2010**, *44*, 8128. doi:10.1021/ES101698Q

[24] M. C. Facchini, S. Fuzzi, S. Zappoli, A. Andracchio, A. Gelencsér, G. Kiss, Z. Krivácsy, E. Meszaros, H. C. Hansson, T. Alsberg, Y. Zebuhr, Partitioning of the organic aerosol component between fog droplets and interstitial air. *J. Geophys. Res. – Atmos.* **1999**, *104*(D21), 26 821. doi:10.1029/1999JD900349

[25] Z. Krivácsy, G. Kiss, B. Varga, I. Galambos, Z. Sárvári, A. Gelencsér, Á. Molnár, S. Fuzzi, M. C. Facchini, S. Zappoli, A. Andracchio, T. Alsberg, H. C. Hansson, L. Persson, Study of humic-like substances in fog and interstitial aerosol by size-exclusion chromatography and

capillary electrophoresis. *Atmos. Environ.* **2000**, *34*, 4273. doi:10.1016/S1352-2310(00)00211-9

[26] G. Kiss, B. Varga, A. Gelencser, Z. Krivacsy, A. Molnar, T. Alsberg, L. Persson, H. C. Hansson, M. C. Facchini, Characterisation of polar organic compounds in fog water. *Atmos. Environ.* **2001**, *35*, 2193. doi:10.1016/S1352-2310(00)00473-8

[27] S. Fuzzi, M. C. Facchini, S. Decesari, E. Matta, M. Mircea, Soluble organic compounds in fog and cloud droplets: what have we learned over the past few years? *Atmos. Res.* **2002**, *64*, 89. doi:10.1016/S0169-8095(02)00082-0

[28] P. Herckes, T. Lee, L. Trenary, G. G. Kang, H. Chang, J. L. Collett Jr, Organic matter in central California radiation fogs. *Environ. Sci. Technol.* **2002**, *36*, 4777. doi:10.1021/ES025889T

[29] A. Cappiello, E. De Simoni, C. Fiorucci, F. Mangani, P. Palma, H. Trufelli, S. Decesari, M. C. Facchini, S. Fuzzi, Molecular characterization of the water-soluble organic compounds in fogwater by ESIMS/MS. *Environ. Sci. Technol.* **2003**, *37*, 1229. doi:10.1021/ES0259990

[30] J. L. Collett Jr, P. Herckes, S. Youngster, T. Lee, Processing of atmospheric organic matter by California radiation fogs. *Atmos. Res.* **2008**, *87*, 232. doi:10.1016/J.ATMOSRES.2007.11.005

[31] S. Raja, R. Raghunathan, R. R. Kommalapati, X. H. Shen, J. L. Collett Jr, K. T. Valsaraj, Organic composition of fogwater in the Texas–Louisiana gulf coast corridor. *Atmos. Environ.* **2009**, *43*, 4214. doi:10.1016/J.ATMOSENV.2009.05.029

[32] P. Herckes, M. P. Hannigan, L. Trenary, T. Lee, J. L. Collett Jr, Organic compounds in radiation fogs in Davis (California). *Atmos. Res.* **2002**, *64*, 99. doi:10.1016/S0169-8095(02)00083-2

[33] P. Herckes, J. A. Leenheer, J. L. Collett Jr, Comprehensive characterization of atmospheric organic matter in Fresno, California, fog water. *Environ. Sci. Technol.* **2007**, *41*, 393. doi:10.1021/ES0607988

[34] L. R. Mazzoleni, B. M. Ehrmann, X. Shen, A. G. Marshall, J. L. Collett Jr, Water-soluble atmospheric organic matter in fog: exact masses and chemical formula identification by ultrahigh-resolution Fourier transform ion cyclotron resonance mass spectrometry. *Environ. Sci. Technol.* **2010**, *44*, 3690. doi:10.1021/ES903409K

[35] A. Nel, Air pollution-related illness: effects of particles. *Science* **2005**, *308*, 804. doi:10.1126/SCIENCE.1108752

[36] J. Haywood, O. Boucher, Estimates of the direct and indirect radiative forcing due to tropospheric aerosols: a review. *Rev. Geophys.* **2000**, *38*, 513. doi:10.1029/1999RG000078

[37] Q. Zhang, J. L. Jimenez, M. R. Canagaratna, J. D. Allan, H. Coe, I. Ulbrich, M. R. Alfarra, A. Takami, A. M. Middlebrook, Y. L. Sun, K. Dzepina, E. Dunlea, K. Docherty, P. F. DeCarlo, D. Salcedo, T. Onasch, J. T. Jayne, T. Miyoshi, A. Shimono, S. Hatakeyama, N. Takegawa, Y. Kondo, J. Schneider, F. Drewnick, S. Borrmann, S. Weimer, K. Demerjian, P. Williams, K. Bower, R. Bahreini, L. Cottrell, R. J. Griffin, J. Rautiainen, J. Y. Sun, Y. M. Zhang, D. R. Worsnop, Ubiquity and dominance of oxygenated species in organic aerosols in anthropogenically influenced northern hemisphere midlatitudes. *Geophys. Res. Lett.* **2007**, *34*, L13801. doi:10.1029/2007GL029979

[38] N. L. Ng, M. R. Canagaratna, Q. Zhang, J. L. Jimenez, J. Tian, I. M. Ulbrich, J. H. Kroll, K. S. Docherty, P. S. Chhabra, R. Bahreini, S. M. Murphy, J. H. Seinfeld, L. Hildebrandt, N. M. Donahue, P. F. DeCarlo, V. A. Lanz, A. S. H. Prevot, E. Dinar, Y. Rudich, D. R. Worsnop, Organic aerosol components observed in northern hemispheric datasets from aerosol mass spectrometry. *Atmos. Chem. Phys.* **2010**, *10*, 4625. doi:10.5194/ACP-10-4625-2010

[39] J. L. Jimenez, M. R. Canagaratna, N. M. Donahue, A. S. H. Prevot, Q. Zhang, J. H. Kroll, P. F. DeCarlo, J. D. Allan, H. Coe, N. L. Ng, A. C. Aiken, K. S. Docherty, I. M. Ulbrich, A. P. Grieshop, A. L. Robinson, J. Duplissy, J. D. Smith, K. R. Wilson, V. A. Lanz, C. Hueglin, Y. L. Sun, J. Tian, A. Laaksonen, T. Raatikainen, J. Rautiainen, P. Vaattovaara, M. Ehn, M. Kulmala, J. M. Tomlinson, D. R. Collins, M. J. Cubison, E. J. Dunlea, J. A. Huffman, T. B. Onasch, M. R. Alfarra, P. I. Williams, K. Bower, Y. Kondo, J. Schneider, F. Drewnick, S. Borrmann, S. Weimer, K. Demerjian, D. Salcedo, L. Cottrell, R. Griffin, A. Takami, T. Miyoshi, S. Hatakeyama, A. Shimono, J. Y. Sun, Y. M. Zhang, K. Dzepina, J. R. Kimmel, D. Sueper, J. T. Jayne, S. C. Herndon, A. M. Trimborn, L. R. Williams, E. C. Wood, A. M. Middlebrook, C. E. Kolb, U. Baltensperger, D. R. Worsnop, Evolution of organic aerosols in the atmosphere. *Science* **2009**, *326*, 1525. doi:10.1126/SCIENCE.1180353

[40] Q. Zhang, J. Jimenez, M. Canagaratna, I. Ulbrich, N. Ng, D. Worsnop, Y. Sun, Understanding atmospheric organic aerosols via factor analysis of aerosol mass spectrometry: a review. *Anal. Bioanal. Chem.* **2011**, *401*, 3045. doi:10.1007/S00216-011-5355-Y

[41] M. Dall'Osto, R. M. Harrison, H. Coe, P. Williams, Real-time secondary aerosol formation during a fog event in London. *Atmos. Chem. Phys.* **2009**, *9*, 2459. doi:10.5194/ACP-9-2459-2009

[42] C. M. Berkowitz, L. K. Berg, X.-Y. Yu, M. L. Alexander, A. Laskin, R. A. Zaveri, B. T. Jobson, E. Andrews, J. A. Ogren, The influence of fog and airmass history on aerosol optical, physical and chemical properties at Pt Reyes National Seashore. *Atmos. Environ.* **2011**, *45*, 2559. doi:10.1016/J.ATMOSENV.2011.02.016

[43] K. J. Hoag, J. L. Collett Jr, S. N. Pandis, The influence of drop size-dependent fog chemistry on aerosol processing by San Joaquin Valley fogs. *Atmos. Environ.* **1999**, *33*, 4817. doi:10.1016/S1352-2310(99)00268-X

[44] W. A. Ham, J. D. Herner, P. G. Green, M. J. Kleeman, Size distribution of health-relevant trace elements in airborne particulate matter during a severe winter stagnation event: implications for epidemiology and inhalation exposure studies. *Aerosol Sci. Technol.* **2010**, *44*, 753. doi:10.1080/02786826.2010.488660

[45] W. A. Ham, C. R. Ruehl, M. J. Kleeman, Seasonal variation of airborne particle deposition efficiency in the human respiratory system. *Aerosol Sci. Technol.* **2011**, *45*, 795. doi:10.1080/02786826.2011.564239

[46] A. K. Madl, K. E. Pinkerton, Health effects of inhaled engineered and incidental nanoparticles. *Crit. Rev. Toxicol.* **2009**, *39*, 629. doi:10.1080/10408440903133788

[47] K. J. Bein, Y. Zhao, A. S. Wexler, Conditional sampling for source-oriented toxicological studies using a single particle mass spectrometer. *Environ. Sci. Technol.* **2009**, *43*, 9445. doi:10.1021/ES901966A

[48] M. R. Canagaratna, J. T. Jayne, J. L. Jimenez, J. D. Allan, M. R. Alfarra, Q. Zhang, T. B. Onasch, F. Drewnick, H. Coe, A. Middlebrook, A. Delia, L. R. Williams, A. M. Trimborn, M. J. Northway, P. F. DeCarlo, C. E. Kolb, P. Davidovits, D. R. Worsnop, Chemical and microphysical characterization of ambient aerosols with the aerodyne aerosol mass spectrometer. *Mass Spectrom. Rev.* **2007**, *26*, 185. doi:10.1002/MAS.20115

[49] P. F. DeCarlo, J. R. Kimmel, A. Trimborn, M. J. Northway, J. T. Jayne, A. C. Aiken, M. Gonin, K. Fuhrer, T. Horvath, K. S. Docherty, D. R. Worsnop, J. L. Jimenez, Field-deployable, high-resolution, time-of-flight aerosol mass spectrometer. *Anal. Chem.* **2006**, *78*, 8281. doi:10.1021/AC061249N

[50] Q. Zhang, M. R. Canagaratna, J. T. Jayne, D. R. Worsnop, J. L. Jimenez, Time- and size-resolved chemical composition of submicron particles in Pittsburgh: implications for aerosol sources and processes. *J. Geophys. Res. – Atmos.* **2005**, *110*(D7), D07S09. doi:10.1029/2004JD004649

[51] J. D. Allan, A. E. Delia, H. Coe, K. N. Bower, M. R. Alfarra, J. L. Jimenez, A. M. Middlebrook, F. Drewnick, T. B. Onasch, M. R. Canagaratna, J. T. Jayne, D. R. Worsnop, A generalised method for the extraction of chemically resolved mass spectra from aerodyne aerosol mass spectrometer data. *J. Aerosol Sci.* **2004**, *35*, 909. doi:10.1016/J.JAEROSCI.2004.02.007

[52] A. C. Aiken, P. F. Decarlo, J. H. Kroll, D. R. Worsnop, J. A. Huffman, K. S. Docherty, I. M. Ulbrich, C. Mohr, J. R. Kimmel, D. Sueper, Y. Sun, Q. Zhang, A. Trimborn, M. Northway, P. J. Ziemann, M. R. Canagaratna, T. B. Onasch, M. R. Alfarra, A. S. H. Prévôt, J. Dommen, J. Duplissy, A. Metzger, U. Baltensperger, J. L. Jimenez, O/C and OM/OC ratios of primary, secondary, and ambient organic aerosols with high-resolution time-of-flight aerosol mass spectrometry. *Environ. Sci. Technol.* **2008**, *42*, 4478. doi:10.1021/ES703009Q

[53] A. M. Middlebrook, R. Bahreini, J. L. Jimenez, M. R. Canagaratna, Evaluation of composition-dependent collection efficiencies for the aerodyne aerosol mass spectrometer using field data. *Aerosol Sci. Technol.* **2012**, *46*, 258. doi:10.1080/02786826.2011.620041

[54] P. F. DeCarlo, J. G. Slowik, D. R. Worsnop, P. Davidovits, J. L. Jimenez, Particle morphology and density characterization by combined mobility and aerodynamic diameter measurements. Part 1. Theory. *Aerosol Sci. Technol.* **2004**, *38*, 1185.

[55] E. S. Cross, J. G. Slowik, P. Davidovits, J. D. Allan, D. R. Worsnop, J. T. Jayne, D. K. Lewis, M. Canagaratna, T. B. Onasch, Laboratory and ambient particle density determinations using light scattering in conjunction with aerosol mass spectrometry. *Aerosol Sci. Technol.* **2007**, *41*, 343. doi:10.1080/02786820701199736

[56] I. M. Ulbrich, M. R. Canagaratna, Q. Zhang, D. R. Worsnop, J. L. Jimenez, Interpretation of organic components from positive matrix factorization of aerosol mass spectrometric data. *Atmos. Chem. Phys.* **2009**, *9*, 2891. doi:10.5194/ACP-9-2891-2009

[57] P. Paatero, U. Tapper, Positive matrix factorization: a non-negative factor model with optimal utilization of error estimates of data values. *Environmetrics* **1994**, *5*, 111. doi:10.1002/ENV.3170050203

[58] S. H. Chu, J. W. Paisie, B. W. L. Jang, PM data analysis – a comparison of two urban areas: Fresno and Atlanta. *Atmos. Environ.* **2004**, *38*, 3155. doi:10.1016/J.ATMOSENV.2004.03.018

[59] R. V. Mallina, A. S. Wexler, M. V. Johnston, Particle growth in high-speed particle beam inlets. *J. Aerosol Sci.* **1997**, *28*, 223. doi:10.1016/S0021-8502(96)00435-1

[60] J. L. Collett Jr, K. J. Hoag, X. Rao, Internal acid buffering in San Joaquin Valley fog drops and its influence on aerosol processing. *Atmos. Environ.* **1999**, *33*, 4833. doi:10.1016/S1352-2310(99)00221-6

[61] F. W. Lurmann, S. G. Brown, M. C. McCarthy, P. T. Roberts, Processes influencing secondary aerosol formation in the San Joaquin Valley during winter. *J. Air Waste Manage.* **2006**, *56*, 1679. doi:10.1080/10473289.2006.10464573

[62] K. Turkiewicz, K. Magliano, T. Najita, Comparison of two winter air quality episodes during the California regional particulate air quality study. *J. Air Waste Manage.* **2006**, *56*, 467. doi:10.1080/10473289.2006.10464525

[63] J. C. Chow, J. G. Watson, D. H. Lowenthal, K. L. Magliano, Size-resolved aerosol chemical concentrations at rural and urban sites in central California, USA. *Atmos. Res.* **2008**, *90*, 243. doi:10.1016/J.ATMOSRES.2008.03.017

[64] J. C. Chow, J. G. Watson, D. H. Lowenthal, R. Hackney, K. Magliano, D. Lehrman, T. Smith, Temporal variations of $PM_{2.5}$, PM_{10}, and gaseous precursors during the 1995 integrated monitoring study in central California. *J. Air Waste Manage. Assoc.* **1999**, *49*, 16. doi:10.1080/10473289.1999.10463909

[65] Q. Zhang, D. R. Worsnop, M. R. Canagaratna, J. L. Jimenez, Hydrocarbon-like and oxygenated organic aerosols in Pittsburgh: insights into sources and processes of organic aerosols. *Atmos. Chem. Phys.* **2005**, *5*, 3289. doi:10.5194/ACP-5-3289-2005

[66] B. Ervens, B. J. Turpin, R. J. Weber, Secondary organic aerosol formation in cloud droplets and aqueous particles (aqSOA): a review of laboratory, field and model studies. *Atmos. Chem. Phys.* **2011**, *11*, 11 069. doi:10.5194/ACP-11-11069-2011

[67] Y. L. Sun, Q. Zhang, J. J. Schwab, W. N. Chen, M. S. Bae, Y. C. Lin, H. M. Hung, K. L. Demerjian, A case study of aerosol processing and evolution in summer in New York City. *Atmos. Chem. Phys.* **2011**, *11*, 12 737. doi:10.5194/ACP-11-12737-2011

[68] S. V. Hering, S. K. Friedlander, Origins of aerosol sulfur size distributions in the Los Angeles basin. *Atmos. Environ.* **1982**, *16*, 2647. doi:10.1016/0004-6981(82)90346-8

[69] W. John, S. M. Wall, J. L. Ondo, W. Winklmayr, Modes in the size distributions of atmospheric inorganic aerosol. *Atmos. Environ., A Gen. Topics* **1990**, *24*, 2349. doi:10.1016/0960-1686(90)90327-J

[70] Z. Meng, J. H. Seinfeld, On the source of the submicrometer droplet mode of urban and regional aerosols. *Aerosol Sci. Technol.* **1994**, *20*, 253. doi:10.1080/02786829408959681

[71] V.-M. Kerminen, A. S. Wexler, Growth laws for atmospheric aerosol particles: an examination of the bimodality of the accumulation mode. *Atmos. Environ.* **1995**, *29*, 3263. doi:10.1016/1352-2310(95)00249-X

[72] J. D. Blando, B. J. Turpin, Secondary organic aerosol formation in cloud and fog droplets: a literature evaluation of plausibility. *Atmos. Environ.* **2000**, *34*, 1623. doi:10.1016/S1352-2310(99)00392-1

[73] R. Volkamer, F. San Martini, L. T. Molina, D. Salcedo, J. L. Jimenez, M. J. Molina, A missing sink for gas-phase glyoxal in Mexico City: formation of secondary organic aerosol. *Geophys. Res. Lett.* **2007**, *34*, L19807. doi:10.1029/2007GL030752

[74] R. Volkamer, P. J. Ziemann, M. J. Molina, Secondary organic aerosol formation from acetylene (C_2H_2): seed effect on SOA yields due to organic photochemistry in the aerosol aqueous phase. *Atmos. Chem. Phys.* **2009**, *9*, 1907. doi:10.5194/ACP-9-1907-2009

[75] Y. L. Sun, Q. Zhang, M. Zheng, X. Ding, E. S. Edgerton, X. Wang, Characterization and source apportionment of water-soluble organic matter in atmospheric fine particles ($PM_{2.5}$) with high-resolution aerosol mass spectrometry and GC–MS. *Environ. Sci. Technol.* **2011**, *45*, 4854. doi:10.1021/ES200162H

[76] D. S. Kaul, T. Gupta, S. N. Tripathi, V. Tare, J. L. Collett Jr, Secondary organic aerosol: a comparison between foggy and nonfoggy days. *Environ. Sci. Technol.* **2011**, *45*, 7307. doi:10.1021/ES201081D

[77] S. R. Zorn, F. Drewnick, M. Schott, T. Hoffmann, S. Borrmann, Characterization of the south Atlantic marine boundary layer aerosol using an aerodyne aerosol mass spectrometer. *Atmos. Chem. Phys.* **2008**, *8*, 4711. doi:10.5194/ACP-8-4711-2008

[78] R. von Glasow, P. J. Crutzen, Model study of multiphase DMS oxidation with a focus on halogens. *Atmos. Chem. Phys.* **2004**, *4*, 589. doi:10.5194/ACP-4-589-2004

[79] L. Phinney, W. Richard Leaitch, U. Lohmann, H. Boudries, D. R. Worsnop, J. T. Jayne, D. Toom-Sauntry, M. Wadleigh, S. Sharma, N. Shantz, Characterization of the aerosol over the Sub-Arctic North East Pacific Ocean. *Deep Sea Res. Part II Top. Stud. Oceanogr.* **2006**, *53*, 2410. doi:10.1016/J.DSR2.2006.05.044

[80] C. J. Gaston, K. A. Pratt, X. Qin, K. A. Prather, Real-time detection and mixing state of methanesulfonate in single particles at an inland urban location during a phytoplankton bloom. *Environ. Sci. Technol.* **2010**, *44*, 1566. doi:10.1021/ES902069D

[81] J. A. Huffman, K. S. Docherty, A. C. Aiken, M. J. Cubison, I. M. Ulbrich, P. F. DeCarlo, D. Sueper, J. T. Jayne, D. R. Worsnop, P. J. Ziemann, J. L. Jimenez, Chemically resolved aerosol volatility measurements from two megacity field studies. *Atmos. Chem. Phys.* **2009**, *9*, 7161. doi:10.5194/ACP-9-7161-2009

[82] S. F. Watts, The mass budgets of carbonyl sulfide, dimethyl sulfide, carbon disulfide and hydrogen sulfide. *Atmos. Environ.* **2000**, *34*, 761. doi:10.1016/S1352-2310(99)00342-8

[83] H. Schäfer, N. Myronova, R. Boden, Microbial degradation of dimethylsulphide and related c1-sulphur compounds: organisms and pathways controlling fluxes of sulphur in the biosphere. *J. Exp. Bot.* **2010**, *61*, 315. doi:10.1093/JXB/ERP355

[84] I. Barnes, J. Hjorth, N. Mihalopoulos, Dimethyl sulfide and dimethyl sulfoxide and their oxidation in the atmosphere. *Chem. Rev.* **2006**, *106*, 940. doi:10.1021/CR020529+

[85] J. R. Whiteaker, K. A. Prather, Hydroxymethanesulfonate as a tracer for fog processing of individual aerosol particles. *Atmos. Environ.* **2003**, *37*, 1033. doi:10.1016/S1352-2310(02)01029-4

[86] S. H. Lee, D. M. Murphy, D. S. Thomson, A. M. Middlebrook, Nitrate and oxidized organic ions in single particle mass spectra during the 1999 Atlanta supersite project. *J. Geophys. Res. – Atmos.* **2003**, *108* (D7), 8417. doi:10.1029/2001JD001455

[87] Q. Zhang, J. L. Jimenez, D. R. Worsnop, M. Canagaratna, A case study of urban particle acidity and its influence on secondary organic aerosol. *Environ. Sci. Technol.* **2007**, *41*, 3213. doi:10.1021/ES061812J